PASJ: Publ. Astron. Soc. Japan **51**, 81–90 (1999)

Optical Number Count Estimation of IRIS Far-Infrared Survey of Galaxies

Hiroyuki HIRASHITA,* Tsutomu T. TAKEUCHI,* and Kouji OHTA
Department of Astronomy, Faculty of Science, Kyoto University, Sakyo-ku, Kyoto 606-8502
E-mail (HH): hirasita@kusastro.kyoto-u.ac.jp
and
Hiroshi SHIBAI
Department of Physics, Nagoya University, Chikusa-ku, Nagoya 464-8602

(Received 1998 June 15; accepted 1998 December 1)

Abstract

Infrared Imaging Surveyor (IRIS) is a satellite which will be launched at the beginning of 2003. One of the main purposes of the IRIS mission is an all-sky survey in the far-infrared region with a flux limit much deeper than that of IRAS. The detection of a large number of galaxies ($\sim$ several $\times 10^6$ in the whole sky) is expected in this survey. We investigated the expected optical and near-infrared (NIR) number counts of galaxies detected by the far-infrared scanner (FIS) of IRIS (hereafter, IRIS galaxies) and the possibility of their optical and NIR follow-up. The spectral energy distribution and the luminosity function of the IRIS galaxies are modeled based on the properties of galaxies observed by IRAS. The IRIS galaxies are divided into two populations according to their infrared luminosities ($L_{\rm IR}$): normal spirals ($L_{\rm IR} < 10^{10}\,L_\odot$) and starbursts ($L_{\rm IR} > 10^{10}\,L_\odot$). The expected number counts of IRIS galaxies for both of the populations are calculated in B and H bands. We show that about 60 normal galaxies and about 80 starburst galaxies are detected per square degree in both of the two bands, when galaxy evolution is not taken into account. All of the normal population of IRIS galaxies are located at the redshift $z \lesssim 0.1$. As for the starburst population, we also calculated the number of galaxies with a simple model of evolution. The total number of starburst population predicted by the evolution model is larger by 20% than that expected from the non-evolution model. In the evolution model, the numbers of low-z ($z < 1$), intermediate-z ($1 < z < 3$), and high-z ($z > 3$) galaxies are 100, 20, and 0.2 per square degree, respectively.

Key words: Cosmology — Galaxies: evolution — Infrared: spectra — Interstellar: dust

1. Introduction

There have been a number of advances in understanding galaxy evolution over the last few years by optical redshift surveys of galaxies (e.g., Lilly et al. 1995; Cowie et al. 1996; Ellis et al. 1996; Hammer et al. 1997; Heyl et al. 1997; Small et al. 1997). These surveys have been revealing the star-formation history of the Universe up to $z \sim 1$. The star-formation rate around $z = 1$ is found to be several times larger than that at $z = 0$. The Lyman-break technique also provides the star-formation properties of galaxies at around $z = 3$ based on the rest ultraviolet (UV) light (e.g., Steidel et al. 1996), and the star-formation rate in the Universe seems to have a peak at $z \sim 1$–2 (Madau et al. 1996). However, optical and UV light may severely suffer from extinction by dust.

The far-infrared (FIR) is another important wavelength to trace the star-formation history of the Universe, because the energy absorbed by dust at UV and optical regions is re-emitted in FIR and extinction in FIR is very small. Furthermore, for starburst galaxies, the bulk of the energy is released in FIR; the survey by the Infrared Astronomical Satellite (IRAS) discovered hundreds of galaxies emitting well over 95% of their total luminosity in the infrared (e.g., Soifer et al. 1987a). Thus, surveys only in UV and optical wavelengths are not sufficient to clarify the star-formation history of the Universe. We also need to investigate the star-formation history in the FIR bands.

In the FIR wavelengths, galaxy evolution is discussed based on the number count of the IRAS all-sky survey with a flux limit of $\sim$ 1 Jy at 60 μm. Hacking et al. (1987) and Saunders et al. (1990) showed that the observed counts of faint 60-μm sources are about twice as high as the non-evolutionary model prediction, suggesting the presence of source evolution. However, since the depth of the IRAS survey is only $z \sim 0.1$ in median (Sanders, Mirabel 1996), a deeper survey is indispensable

* Research Fellow of the Japan Society for the Promotion of Science.

Table 1. Flux limits of the IRIS far-infrared scanner.

Wavelength [μm]	5σ-detection limit [mJy]
50	20
70	15
120	30
150	50

to explore the higher redshift Universe. A survey much deeper than the IRAS survey was performed with the Infrared Space Observatory (ISO; Kessler et al. 1996) at the Lockman Hole with a flux limit of 45 mJy at 175 μm (Kawara et al. 1998). According to Kawara et al. (1998), the surface density of sources brighter than 150 mJy at 175 μm agrees with the model by Guiderdoni et al. (1997), who took into account the burst of star formation whose timescale of gas consumption ($\sim$ 1 Gyr) is ten-times smaller than that observed in normal disk galaxies (Kennicutt et al. 1994). Although this ISO survey is much deeper than the IRAS survey, it covers only a small solid angle of the sky (1600 square arcmin); thus a much wider coverage is clearly necessary in the next step to obtain a huge sample.

The Infrared Imaging Surveyor (IRIS; Astro-F — the project name of IRIS) will be launched at the beginning of the year 2003. A far-infrared scanner (FIS) as well as a near- and mid-infrared camera (IRC) is planned to be onboard. A point source survey in the whole sky will be carried out by FIS with a depth of 15–50 mJy at 50–180 μm (Kawada 1998). Since the flux limit (table 1) is more than 20-times deeper than that of IRAS, the IRIS survey is expected to detect an enormous number of galaxies ($\sim$ several $\times 10^6$ in the whole sky; Takeuchi et al. 1999a, hereafter T99). This survey will contribute to studying the star-formation history and detecting primeval galaxies at high redshift. The survey, however, will not be able to determine the precise redshift (distance) of the detected objects. In order to obtain the redshift and to know the natures of the detected sources (e.g., galactic objects, star-forming galaxies, or AGNs), optical or near-infrared (NIR) follow-up observations are indispensable. Follow-ups will enable us to obtain a systematic and homogeneous large database that will be more useful for studying the evolution of star-forming galaxies and AGNs as well as the properties of large-scale structures. In the optical and NIR wavelengths, the SUBARU telescope will be available when the IRIS survey starts. Hence, the instrumental conditions for the follow-up will be excellent and the follow-up of the IRIS survey will be a timely project.

In this paper we consider the feasibility and strategy of the follow-up of the IRIS survey using models and calculations by T99, in which the source count by IRIS is predicted based on the local FIR luminosity function and the empirical spectral energy distributions (SEDs) of nearby galaxies in the FIR-submillimeter wavelengths, with the assumptions of simple functional forms for the evolution (see also Beichman, Helou 1991; Pearson, Rowan-Robinson 1996). The models adopted to calculate the FIR number count by T99 are reviewed in section 2. We then present the expected number count of galaxies detected by IRIS (hereafter referred to as IRIS galaxies) at optical (B) and NIR (H) bands in section 3. Finally, in section 4 we summarize the feasibility and describe the strategy of the follow-up of the IRIS survey. Throughout this paper we adopt a Hubble constant of $H_0 = 75$ km s^{-1} Mpc^{-1} and a deceleration parameter of $q_0 = 0.1$ (the density parameter $\Omega_0 = 0.2$ and the cosmological constant $\Lambda = 0$), unless otherwise stated.

2. Model of FIR Number Count

In this section we review the model used by T99 to calculate the expected number count of the IRIS survey in FIR bands.

2.1. *Spectral Energy Distribution*

The assumed SEDs in T99 consist of two components, cool cirrus and hot starbursts, following Rowan-Robinson and Crawford (1989). The cirrus component represents the dust heated mainly by late-type stars, while the starburst component stands for emission from dust heated by hot early-type stars associated with intense starbursts (e.g., Sanders, Mirabel 1996). The model spectrum of the cirrus component is taken from the galactic interstellar dust model by Désert et al. (1990). In T99, it was assumed that galaxies with $L_{\rm IR} < 10^{10}\,L_\odot$ have only the cirrus component, where $L_{\rm IR}$ is defined as the infrared luminosity integrated in the wavelength range from 3 μm to 1 mm. Galaxies with larger $L_{\rm IR}$ have both the cirrus and starburst components; an infrared luminosity in excess of $10^{10}\,L_\odot$ is assumed to come from the starburst component. The spectrum of the starburst component $L_{{\rm s}\nu}$ is composed of two-temperature modified blackbody radiation, $L_{{\rm s}\nu} = \alpha\nu B_\nu(T_{\rm cool}) + \beta\nu B_\nu(T_{\rm hot})$, where $B_\nu(T)$ is the Planck function with temperature T; both α and β are normalizing constants. Here, the temperatures of the two components are given by $T_{\rm cool} = 60(L_{\rm s}/10^{11}\,L_\odot)^{0.1}$ K and $T_{\rm hot} = 175(L_{\rm s}/10^{11}\,L_\odot)^{0.1}$ K, where $L_{\rm s}$ is the luminosity of the starburst component integrated over the range from 3 μm to 1 mm (Beichman, Helou 1991; see also Rieke, Lebofsky 1986; Helou 1986; Soifer et al. 1987a). The normalizing constants α and β are determined so that 70% of the starburst component comes from the cool component and 30% from the hot component (Beichman, Helou 1991). The model SED is scaled

properly to yield the given $L_{\rm IR}$. In the model, AGNs are not considered, since the number of AGNs is expected to be negligible compared with the number of normal and starburst galaxies (Beichman, Helou 1991). Even if the evolution of AGNs is considered, this will also be the case (Pearson 1996).

2.2. *Local Luminosity Function*

The local FIR luminosity function of galaxies is derived from the IRAS data (Soifer et al. 1987b). Since Soifer et al. (1987b) used the FIR luminosity at 60 μm, T99 converted it into their $L_{\rm IR}$ by using their model SEDs. An analytical fitting to the data leads to the following double-power-law form of the luminosity function:

$$\log[\phi_0(L_{\rm IR})] = \begin{cases} 7.9 - 1.0 \log (L_{\rm IR}/L_\odot) \\ \quad \text{for } 10^8\, L_\odot < L_{\rm IR} < 10^{10.3}\, L_\odot; \\ 17.1 - 1.9 \log (L_{\rm IR}/L_\odot) \\ \quad \text{for } 10^{10.3}\, L_\odot < L_{\rm IR} < 10^{14}\, L_\odot; \\ \text{no galaxies} \\ \quad \text{otherwise,} \end{cases} \tag{1}$$

where ϕ_0 is the number density of galaxies in Mpc^{-3} dex^{-1} at $z = 0$.

2.3. *Survey Limit*

IRIS is a survey-type infrared telescope in space. Its major goal is to achieve a whole-sky point source survey in the far-infrared wavelength region with an order-of-magnitude higher sensitivity and higher spatial resolution as well as with a longer wavelength photometric band than those of the IRAS survey.

The flux limit of the all-sky IRIS survey is estimated by Kawada (1998) to be 20 mJy at ~ 50 μm, 15 mJy at ~ 70 μm, 30 mJy at ~ 120 μm, and 50 mJy at ~ 150 μm (table 1). In the shorter wavelength region of 50–110 μm, the sensitivity is limited by both the internal and background noise, while in the longer wavelength range of 110–170 μm the detection limit is constrained by confusion effects of the interstellar cirrus in the Galaxy. Much better point-source detection limits can be expected in a limited sky areas near to the ecliptic poles, where the survey scan will be repeated more than a hundred times. In this paper we adopt a conventional value of the point-source detection limit expected for the all-sky survey.

2.4. *Redshift Distribution of IRIS Galaxies*

Assuming the above SED and luminosity function of galaxies, T99 calculated the redshift distribution of IRIS galaxies which were regarded as point sources there. The redshift distribution per unit solid angle and unit redshift is formulated as

$$\frac{d^2N}{d\Omega dz} = \frac{d^2V}{d\Omega dz} \int_{L_{\rm lim}(z)}^{\infty} \phi(L'_{\rm IR},\, z)\, d\log L'_{\rm IR}, \tag{2}$$

where the effect of evolution is included in the luminosity function at z, $\phi(L'_{\rm IR},\, z)$, and the comoving volume element per str and per z is denoted as $d^2V/d\Omega dz$ (Ω is the solid angle). In equation (2), $L_{\rm lim}(z)$ is the limiting luminosity for the source at z. The limiting luminosities are $10^{11}\, L_\odot$ at $z \sim 0.2$, $10^{12}\, L_\odot$ at $z \sim 1$, and $10^{13}\, L_\odot$ at $z \sim 3$. $L_{\rm lim}(z)$ becomes $10^{14}\, L_\odot$ at $z \sim 5$ so that no galaxies are detected in $z > 5$ due to upper luminosity cutoff of the luminosity function [equation (1)]. The comoving volume element can be expressed in terms of cosmological parameters as

$$\frac{d^2V}{{\rm d}\Omega dz} = \frac{c}{H_0} \frac{d_{\rm L}^2}{(1+z)^3 \sqrt{1+2q_0 z}}, \tag{3}$$

where c is the speed of light and $d_{\rm L}$ is the luminosity distance:

$$d_{\rm L} = \frac{c}{H_0 q_0^2} [z q_0 + (q_0 - 1)(\sqrt{2q_0 z + 1} - 1)]\,. \tag{4}$$

The resultant number count per z in the whole sky is shown in figure 1 for 50-, 70-, 120-, and 150-μm surveys in the case of no evolution. The total number count of the IRIS galaxies integrated over all the redshift range is several times 10^6 in the whole sky at each wavelength. The 120-μm survey is the deepest ($z \sim 5$). Both of the 70- and 150-μm surveys reach $z \sim 4.5$ and the 50-μm survey reaches $z \sim 3.5$. Hence, the 120-μm survey is preferable to detect high-z galaxies. As for lower redshift region, the number at 150 μm is one order of magnitude smaller than the others in the range of $0.2 \lesssim z \lesssim 1$, and the number count at 50 μm is one order of magnitude smaller than the other bands at $z \lesssim 0.2$. The redshift distribution of the IRIS galaxies is discussed further in T99.

2.5. *Treatment of Galaxy Evolution*

For galaxy-evolution models, T99 treated pure luminosity evolution and pure density evolution. In this subsection, we briefly review the method to include the evolution effect.

2.5.1. *Pure luminosity evolution*

The pure luminosity evolution in T99 means that the luminosities of galaxies change as a function of redshift with the functional form of the luminosity function fixed [equation (1)]. The effect of the luminosity evolution of galaxies is so modeled that the luminosities of galaxies increase by a factor $f(z)$ at a redshift z: $L_{\rm IR}(z) = L_{\rm IR}(z=0) f(z)$. The function $f(z)$ is empirically given in T99 as

$$f(z) = \exp\left[Q \frac{\tau(z)}{t_{\rm H}}\right], \tag{5}$$

where Q, $\tau(z)$, and $t_{\rm H}$ are, respectively, a parameter defining the magnitude of evolution, look-back time as a function of z, and the Hubble time $1/H_0$.

2.5.2. Pure density evolution

The pure density evolution in T99 means that only the comoving number density of galaxies changes as a function of redshift with the luminosities of the galaxies fixed. The density evolution is so modeled by using a function $g(z)$ that the comoving number density at z is $g(z)$ times larger than that at $z = 0$: $\phi(z, L_{\rm IR}) = \phi_0(L_{\rm IR})g(z)$, where $\phi(z, L_{\rm IR})$ is the luminosity function in the comoving volume at the redshift of z. For $g(z)$, T99 adopted the functional form similar to $f(z)$ defined in equation (5):

$$g(z) = \exp\left[P\frac{\tau(z)}{t_{\rm H}}\right], \tag{6}$$

where P is a parameter representing the magnitude of the evolution.

2.5.3. Determination of parameters and observational constraints

In T99, each of the evolutionary parameters (P and Q) is determined by a comparison with the IRAS extragalactic source count data. Excluding four statistically poorest points, the values fit best to the data of IRAS Point Source Catalog (Joint IRAS Science Working Group 1985) and of Hacking and Houck (1987) are $P = 2.7$ or $Q = 1.4$ when $q_0 = 0.1$. Recent ISO result at 175 μm by Kawara et al. (1998) is consistent with the model prediction of T99. The cosmic infrared background radiation predicted by the model of T99 is consistent with the DIRBE and FIRAS results (Puget et al. 1996; Fixsen et al. 1998; Hauser et al. 1998) in the FIR region. We note that the submillimeter background radiation predicted by T99 is a few–ten times larger than the DIRBE and FIRAS results. The redshifted dust emission, whose peak is located at 30–100 μm at the rest frame of the galaxy (figure 1 of T99), largely contributes to the submillimeter background. Thus, constraint on the galaxy evolution in the high-redshift Universe from the submillimeter background is suggested to be useful for future work. The model is also compared with the SCUBA data (Smail et al. 1997; Hughes et al. 1998; Barger et al. 1998) in appendix of T99.

3. Number Count of IRIS Galaxies in Optical and NIR Wavelengths

In this section, we estimate the number of the IRIS galaxies for B ($\lambda = 4400$ Å) and H ($\lambda = 16500$ Å) bands. Galaxy evolution is not taken into account at first. The effects of the evolution are considered later in this section.

3.1. Method for Calculation

We calculate the expected numbers of the IRIS galaxies at B and H bands in the following way:

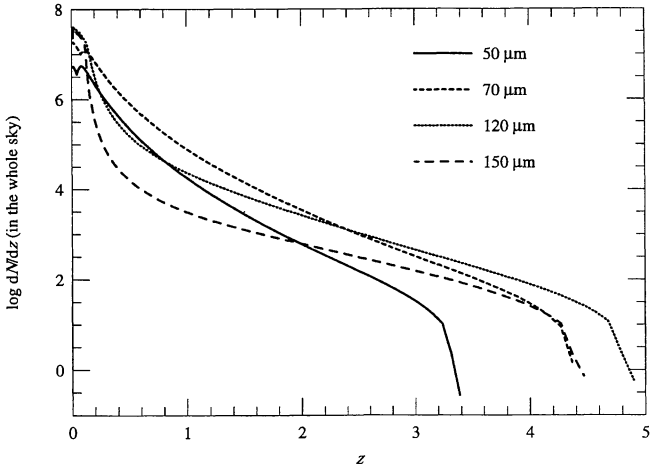

Fig. 1. Number of the IRIS galaxies per unit z. The solid, dashed, dotted, and long-dashed lines represent 50-, 70-, 120-, and 150-μm surveys, respectively.

[1] Two populations for the IRIS galaxies are assumed; starburst population and normal spiral population. We define the starburst population as galaxies whose $L_{\rm IR}$ exceeds $10^{10}\,L_\odot$. This classification of the populations corresponds to two different compositions of FIR SEDs in subsection 2.1.

[2] For the UV-to-FIR SED of each population, we use averaged SEDs of sample galaxies in Schmitt et al. (1997). They collected the nearby galaxies from the catalog of ultraviolet IUE spectra (Kinney et al. 1993, 1996), whose ground-based spectra observed with apartures matching that of IUE ($10'' \times 20''$) were available. The sample contains 6 normal spirals and 26 starburst galaxies. The starburst galaxies are divided into two categories: the high-reddened sample (15 galaxies) and the low-reddened sample (11 galaxies) at $E(B-V) = 0.4$. The reddening was calculated in Calzetti et al. (1994) from Balmer decrement with Seaton's reddening law (Seaton 1979). In this work, we used the high-reddened sample, so that the UV or optical luminosity density converted from the FIR luminosity density gives fainter estimation. The conversion of $L_{\rm IR}$ to the luminosity for each band (at frequency ν) is made for the two populations using the averaged SEDs as $\mathcal{L}_\nu/\mathcal{L}_{60\,\mu{\rm m}} = \alpha_\nu$, where $\mathcal{L}_\nu = \nu L_\nu$. We should note that $\mathcal{L}_{60\,\mu{\rm m}}$ and $L_{\rm IR}$ are related to each other (subsection 2.2). The value of α_ν, which is assumed to be a function of ν only, is listed in table 2 for each population and wavelength. The ratio of luminosity density at ν to that at 60 μm is kept constant for each population. We should keep in mind that the scatter of α_ν is large (an order of magnitude) in observational data. Since our estimation is made for FIR-selected sample, use of SEDs in Spinoglio et al. (1995),

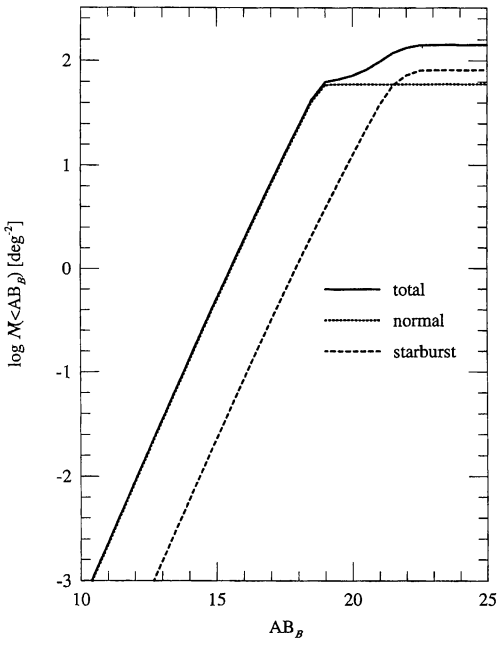

Fig. 2a. Cumulative number count of the IRIS galaxies in the B band (per square degree). The dotted and dashed lines represent the number of normal and starburst populations, respectively. The total number count is also shown (the solid line).

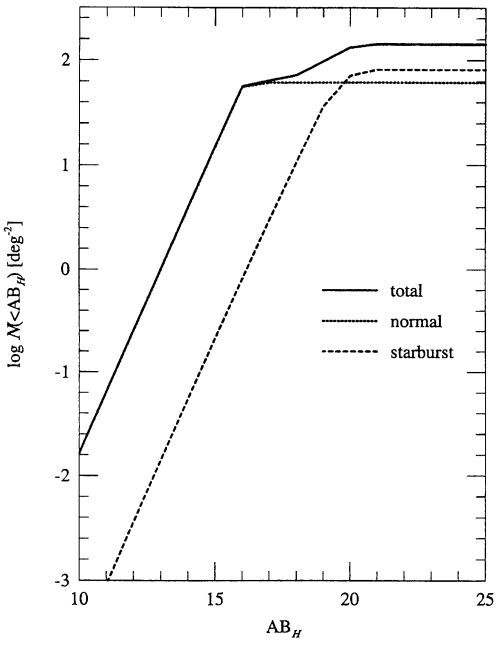

Fig. 2b. Same as figure 2a, but in the H band.

Table 2. Parameter (α) for the conversion of luminosities.

Population (band)	α^*
Starburst (B)	0.10
Normal (B)	4.0
Starburst (H)	0.12
Normal (H)	10

*$\alpha = \mathcal{L}_\nu/\mathcal{L}_{60\mu\mathrm{m}}$, where $\mathcal{L}_\nu = \nu L_\nu$ (L_ν is luminosity density of a galaxy).

in which the sample was selected at 12 μm, is better. However, we need UV data to evaluate the optical magnitude of galaxies at high redshift, and thus we used the data in Schmitt et al. (1997). It is worth noting that the FIR-to-optical SEDs of 12-μm sample in Spinoglio et al. (1995; their figure 11) is consistent with the value of α_ν in table 1 within an order of magnitude, typical scatter of the data in Schmitt et al. (1997). A comment on the SEDs can be seen in subsection 5.2 of Takeuchi et al. (1999b).

[3] The local luminosity function $\phi_0(AB_\nu)$ (Mpc^{-3} mag^{-1}) is made based on Soifer et al. (1987b) by using the above conversion of the luminosity density. The definition of the AB mag (AB_ν) is given by Oke and Gunn (1983); $AB_\nu(\mathrm{mag}) = -2.5\log f_\nu$ (erg cm^{-2} s^{-1} Hz^{-1}) $- 48.594$ ($B = AB + 0.2$; $H = AB - 1.4$). The B-band luminosity function is described as follows. For the normal population,

$$\log\phi_0\ (\mathrm{Mpc}^{-3}\ \mathrm{mag}^{-1}) = 5.08 + 0.38AB_{B,\mathrm{abs}},$$
$$(-19.8 < AB_{B,\mathrm{abs}} < -14.8). \quad (7)$$

where ϕ_0 is the local number density of the IRIS galaxies per magnitude, and the subscript "abs" refers to absolute magnitude. The upper and lower luminosity correspond to $L_{\mathrm{IR}} = 10^{10}\,L_\odot$ ($\mathcal{L}_{60\,\mu\mathrm{m}} = 10^{9.2}\,L_\odot$) and $L_{\mathrm{IR}} = 10^{8}\,L_\odot$ ($\mathcal{L}_{60\,\mu\mathrm{m}} = 10^{7.2}\,L_\odot$), respectively. For the starburst population, double-power-law fitting is executed as follows:

$$\log\phi_0\ (\mathrm{Mpc}^{-3}\ \mathrm{mag}^{-1}) = \begin{cases} 0.02+0.16AB_{B,\mathrm{abs}} & (-18.0 < AB_{B,\mathrm{abs}} < -15.8), \\ 12.07+0.83AB_{B,\mathrm{abs}} & (-25.6 < AB_{B,\mathrm{abs}} < -18.0). \end{cases} \quad (8)$$

Here, the boundary values for the luminosity correspond to $L_{\mathrm{IR}} = 10^{14}\,L_\odot$ ($\mathcal{L}_{60\,\mu\mathrm{m}} = 10^{13.2}\,L_\odot$; $AB_{B,\mathrm{abs}} = -25.6$), $L_{\mathrm{IR}} = 10^{10.3}\,L_\odot$ ($\mathcal{L}_{60\,\mu\mathrm{m}} = 10^{10.1}\,L_\odot$; $AB_{B,\mathrm{abs}} = -18.0$) and $L_{\mathrm{IR}} = 10^{10}\,L_\odot$ ($\mathcal{L}_{60\,\mu\mathrm{m}} = 10^{9.2}\,L_\odot$; $AB_{B,\mathrm{abs}} = -15.8$). For H band, the luminosity function of the normal population is

$$\log\phi_0\,(\mathrm{Mpc}^{-3}\ \mathrm{mag}^{-1}) = 6.00 + 0.38AB_{H,\mathrm{abs}}$$
$$(-22.2 < AB_{H,\mathrm{abs}} < -17.2), \quad (9)$$

while the starburst luminosity function is

$$\log\phi_0\ (\mathrm{Mpc}^{-3}\ \mathrm{mag}^{-1})$$

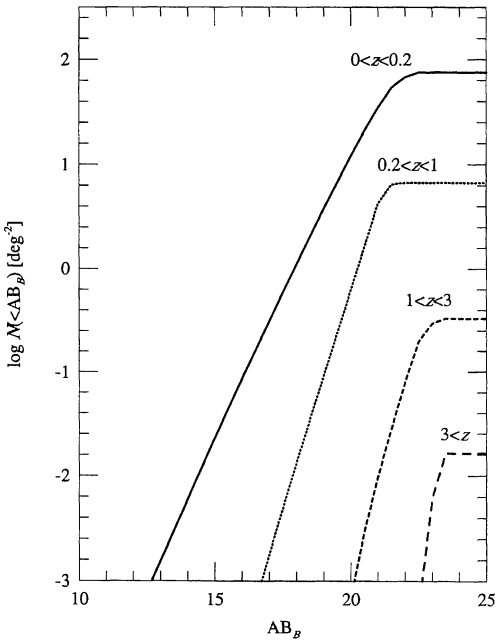

Fig. 3a. Cumulative number counts of the starburst population in various ranges of redshift in the B band. The solid line represents the number count of starbursts in the redshift range of $0 < z < 0.2$, the dotted line $0.2 < z < 1$, the dashed line $1 < z < 3$, and the long-dashed line $3 < z$.

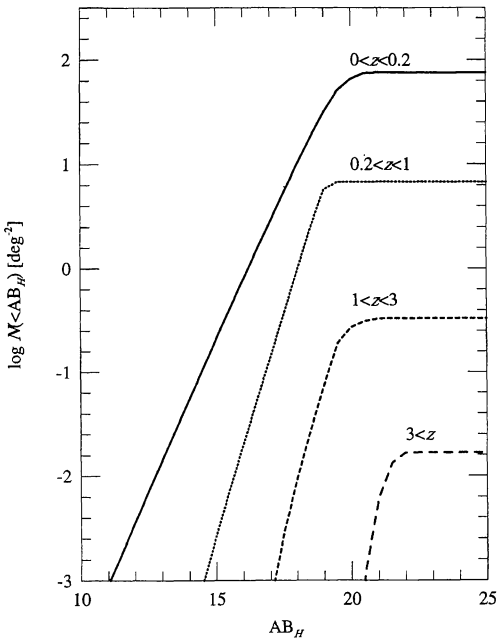

Fig. 3b. Same as figure 3a, but in the H band.

$$= \begin{cases} 0.10+0.15AB_{H,\mathrm{abs}} & (-19.6 < AB_{H,\mathrm{abs}} < -17.4), \\ 13.40+0.83AB_{H,\mathrm{abs}} & (-27.2 < AB_{H,\mathrm{abs}} < -19.6). \end{cases} \quad (10)$$

The fraction of starburst galaxies is 2% of total number of field galaxies at $AB_B \sim -20$ mag (see e.g., Small et al. 1997 for the number density of field galaxies).

[4] The K-corrections, $K(z)$ is expressed by 5-order polynomials fitted to the data of SEDs in Schmitt et al. (1997) as $K(z) = a_1 z + a_2 z^2 + a_3 z^3 + a_4 z^4 + a_5 z^5$. The results of the fitting are presented in table 3. The residual of the fitting of $K(z)$ is less than 0.2 mag in most of the considered z range and 0.5 mag in the worst case; the values are less than the scatter of the luminosity density of the sample in Schmitt et al. (1997).

[5] Finally, the number count of IRIS galaxies per square degree is calculated according to the following formula:

$$N(< AB_\nu) = \oint d\Omega \int_0^\infty dz \int_{AB_{\nu,\mathrm{lim}}(z)}^\infty \times d\,AB_\nu\, \phi(AB_\nu) \frac{d^2V}{dz\, d\Omega}\,, \quad (11)$$

where $AB_{\nu,\mathrm{lim}}(z)$ is the limiting magnitude corresponding to $L_{\mathrm{lim}}(z)$ (subsection 2.4).

3.2. *Results*

The cumulative number counts of IRIS galaxies detected at 120 μm are presented in figures 2a (B band) and 2b (H band). These figures show that number of IRIS galaxies brighter than $AB_B \sim 19$ mag (or $AB_H \sim 16$ mag) increases as the magnitude increases with a slope of 0.6 (dex mag^{-1}), which is the value for the no evolution case in the Euclidean geometry. The figures also show that no IRIS galaxies are detected in the magnitude region fainter than $AB_B \sim 22$ mag (or $AB_H \sim 21$ mag) for starbursts and $AB_B \sim 19$ mag (or $AB_H \sim 16$ mag) for normal spirals. Each of these magnitudes corresponds to optical flux density of each population, which is detected at the flux limit of the IRIS survey. About 60 normal galaxies and 80 starbursts per square degree are detected within this limit. The redshifts of normal spirals are less than 0.1 (T99), as expected from the slope of the counts. In figures 3a and 3b, we also present the number count of starbursts in various redshift range ($z < 0.2$, $0.2 < z < 1$, $1 < z < 3$, and $3 < z$) in the case of the 120-μm survey. About 90% of the starbursts detected by IRIS are located at the redshift of $z < 0.2$ (40% at $z < 0.1$ and 50% at $0.1 < z < 0.2$). For $z \lesssim 3$, the IRIS galaxies are brighter than $AB_B \sim 22$ (or $AB_H \sim 20$), corresponding to the detection limit of IRIS. One high-z ($z > 3$) galaxy exists per ~ 10 square degrees.

We used the high-reddened SED of Schmitt et al. (1997) as that of starburst galaxies (subsection 3.1). The UV-to-FIR ratio of the luminosity density is about

Table 3. The coefficient a_n for the K-correction.

Population (band)	a_1	a_2	a_3	a_4	a_5
Starburst (B)	2.1	−1.2	0.25	-2.3×10^{-2}	7.4×10^{-4}
Normal (B)	5.7	−2.6	−0.39	-1.3×10^{-2}	-4.6×10^{-4}
Starburst (H)	−0.49	0.38	-7.0×10^{-2}	5.2×10^{-3}	-1.4×10^{-4}
Normal (H)	−0.22	0.35	-3.3×10^{-2}	1.1×10^{-4}	3.3×10^{-5}

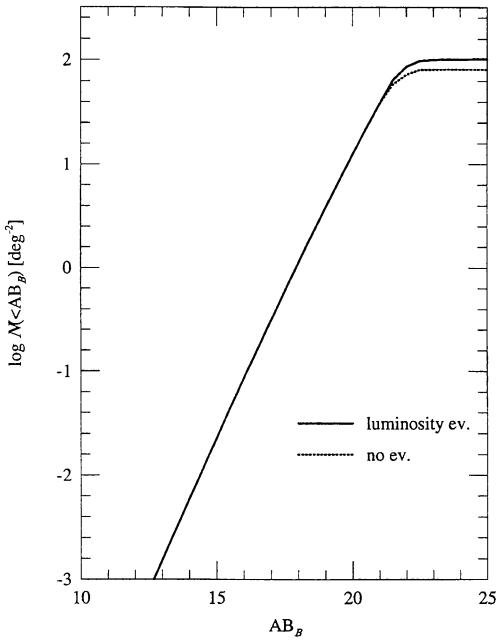

Fig. 4a. Cumulative number count of the starburst population in the B band with our luminosity-evolution model (solid line). The dashed line indicates the count without evolution.

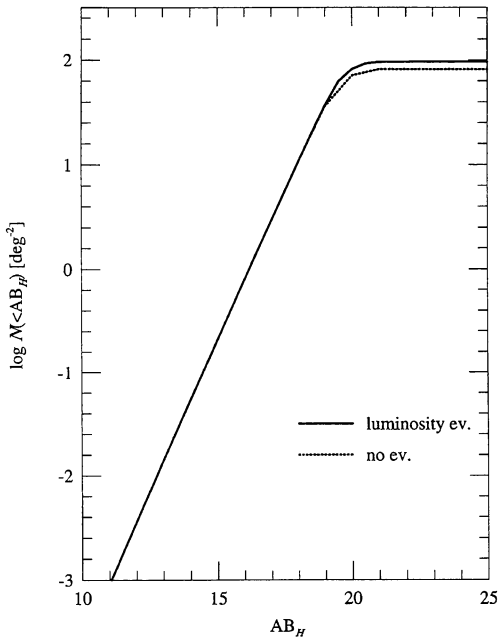

Fig. 4b. Same as figure 4a but in the H band.

2-times larger for the low-reddened SED than for the high-reddened SED. Thus, the optical counterpart of IRIS galaxies may be brighter than expected in this paper by two times (~ 0.8 mag), if the dust extinction is lower. Even if the deceleration parameter of the Universe is not 0.1, but 0.5, there is no significant change in the detected number at $z \lesssim 2$. The number increases by 20% around $z = 3$.

3.3. Effects of Galaxy Evolution

Guiderdoni et al. (1997) calculated the number count of galaxies in FIR wavelength based on models constructed through detailed physical processes related to the evolution of galaxies (see also Franceschini et al. 1994). However, there is a great deal of theoretical uncertainty concerning the physical processes governing galaxy formation and evolution. Thus, we adopt an "empirical approach" (Ellis 1997) based on the luminosity function and SEDs observed in the local universe.

We, here, investigate the pure luminosity evolution in T99. Their model is reviewed in subsection 2.5. The evolution with the parameter $Q = 1.4$, which T99 determined by using IRAS extragalactic source count data, is examined in this paper. This model shows the luminosity evolution of a factor of 1.9 at $z = 1$, 2.4 at $z = 2$, and maintains this evolutionary factor in $z \gtrsim 2$. We assume for simplicity that the luminosity of galaxies evolves in such a way that the ratio of FIR to optical luminosity is kept constant.

Figures 4a and 4b present the effect of evolution for the starburst population. Since almost all of the IRIS galaxies reside in low-z areas, the effect of galaxy evolution is not significant (increase of about 20%). We also present the number count for various range of z in figures 5a and 5b. Comparing figures 3 and 5, we can see that the effect of evolution is significant for high-z galaxies; the number

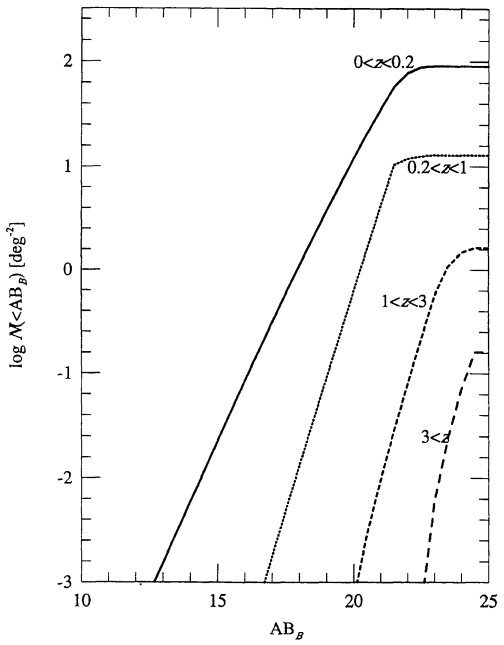

Fig. 5a. Number counts of the starburst population with evolution in various ranges of redshift in the B band (the meaning of the lines are the same as figure 3a).

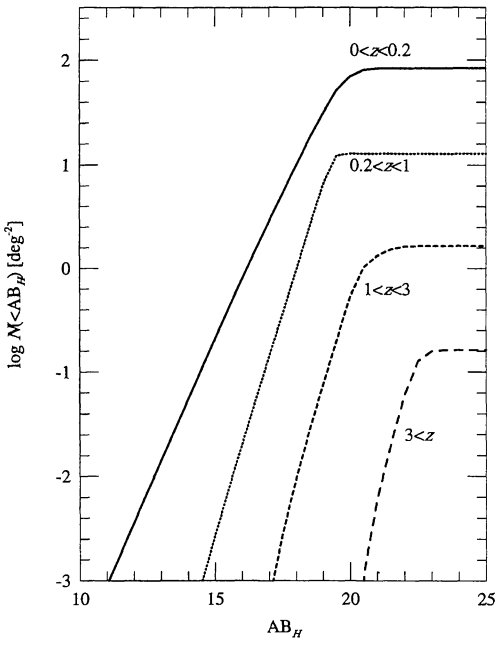

Fig. 5b. Same as figure 5a, but in the H band.

of low-z ($z < 1$), intermediate-z ($1 < z < 3$), and high-z ($z > 3$) galaxies is 100, 20, and 0.2 per square degree, respectively.

The intensity of cosmic infrared background radiation (e.g., Hauser 1995) also constrains the magnitude of galaxy evolution. Since $Q = 1.4$ is almost the upper limit for the magnitude, stronger evolutions with our model break the constraint (T99). The density evolution of the luminosity function in T99 gives almost the same results, since the parameter for the density evolution is determined from the same calibration as that of the luminosity evolution (see T99 for details).

4. Summary and Discussion

We adopted the "empirical approach" model to predict the optical and NIR number counts of galaxies expected to be detected by IRIS. This model is based on the local observed data of IRAS, and is an extension of the IRAS results to a high-z universe. According to our model, such IRIS galaxies have magnitude $AB_\nu \lesssim 21$ at the B and H bands. The expected number of IRIS galaxies at B and H bands per square degree is estimated to be 80 for starburst galaxies and 60 for normal spirals. This value is about 10% of the optical/NIR number count at the same magnitude. As for the redshift distribution, almost all of the normal galaxies are located at $z \lesssim 0.1$, and 40% of the starburst galaxies are at $z < 0.1$, 50% at $0.1 < z < 0.2$, 10% at $0.2 < z < 1$, and 1% at $z > 1$.

By considering the results obtained above together with the effects of the evolutions, the scientific targets of optical/NIR follow-up observations of IRIS galaxies would be twofold. One is to trace star formation properties as well as a large-scale structure of the universe up to $z \sim 1$. The environmental effects on star formation in galaxies will be an important issue. Another target is to find extreme starburst galaxies in a high-z universe, which are in an early stage of galaxy evolution.

IRIS is expected to determine the position of a FIR source with an accuracy of $5''$ (Kawada 1998), which is estimated based on the accuracy of telescope pointing and of fitting to a beam profile. The observed number counts of galaxies in the b_J and K bands show that about 10^{-2} galaxies exist in a $5'' \times 5''$ field at an AB mag of 21 mag (e.g., Broadhurst et al. 1992). This means that a chance coincidence between IRIS galaxies and normal optical galaxies is negligible within this magnitude limit, and thus we can select optical counterpart of IRIS galaxies almost uniquely. Since the expected redshifts of most such IRIS galaxies are low ($z \lesssim 1$), the optical spectroscopy will be good enough to determine the redshifts and natures of the sources. Considering that the number density of IRIS galaxies brighter than $AB_B \simeq 21$ mag is ~ 100 deg^{-2}, a multi-object spectrograph with a wide field of view (such as a fiber multi-object spectrograph) equipped to a 4–8-m class telescope is the best instrument to follow up the IRIS survey. The obtained database will be used to trace the star-formation history

and large scale structures up to $z \sim 1$.

It will be very inefficient to find high-z ultra-luminous FIR galaxies in such a survey described in the previous paragraph because of its very low surface density. We need another approach to obtain a high-z ultra-luminous FIR sample. It is expected that we can make a rough estimate of the redshifts of IRIS galaxies based on a FIR color-color diagram of the sources by using three of IRIS bands, as discussed in T99. Their basic idea is based on the fact that the peaks in the spectra of the thermal radiation from the heated dust at high z is redshifted to a longer wavelength. After selecting the high-z galaxies based on their FIR colors, we need to conduct deep spectroscopic observations which target these objects. Since such high-z objects will have faint magnitude ($AB \lesssim 23$), any optical counterparts may not be uniquely identified; chance probability is not negligible in this magnitude range. Furthermore, "dusty" galaxies may have fainter optical magnitude. Thus, deep multi-slit optical/NIR spectroscopy or the integral field unit of a field of view of $\sim 10''$ will be required. Since making slitlets in a $5''$–$10''$ region would be difficult, the integral field unit would be the most efficient way to identify the FIR source. Hence, integral field units as well as multi-object spectrographs on a 4–8-m class telescope will be powerful tools to conduct optical/NIR follow-ups of the IRIS survey.

We are grateful to the anonymous referee for useful comments which improved our paper. We would like to thank Profs. M. Saitō and S. Mineshige for continuous encouragement. We acknowledge Drs. H. Matsuhara, M. Kawada, and other IRIS staff members for useful discussions and comments. We also thank Drs. T. Yamada, H. Kamaya, T. T. Ishii, and T. G. Hattori for their kind helps and fruitful discussions. Two of the authors (HH and TTT) acknowledge the Research Fellowship of the Japan Society for the Promotion of Science for Young Scientists.

References

Barger A.J., Cowie L.L., Sanders D.B., Fulton E., Taniguchi Y., Sato Y., Kawara K., Okuda H. 1998, Nature 394, 248
Beichman C.A., Helou G. 1991, ApJ 370, L1
Broadhurst T.J., Ellis R.S., Glazebrook K. 1992, Nature 355, 55
Calzetti D., Kinney A.L., Storchi-Bergmann T. 1994, ApJ 429, 582
Cowie L.L., Songaila A., Hu E.M., Cohen J.G. 1996, AJ 112, 839
Désert F.-X., Boulanger F., Puget J.L. 1990, A&A 237, 215
Ellis R.S. 1997, ARA&A 35, 389
Ellis R.S., Colless M., Broadhurst T., Heyl J., Glazebrook K. 1996, MNRAS 280, 235
Fixsen D.J., Dwek E., Mather J.C., Bennett C.L., Shafer R.A. 1998, ApJ 508, 123
Franceschini A., Mazzei P., De Zotti G., Danese L. 1994, ApJ 427, 140
Guiderdoni B., Hivon E., Bouchet F.R., Maffei B. 1997, MNRAS 295, 877
Hacking P., Condon J.J., Houck J.R. 1987, ApJ 316, L15
Hacking P, Houck J.R. 1987, ApJS 63, 311
Hammer F., Flores H., Lilly S.J., Crampton D., Le Fèvre O., Rola C., Mallen-Ornelas G., Schade D. et al. 1997, ApJ 481, 49
Hauser M.G. 1995, in Unveiling the Cosmic Infrared Background, ed E. Dwek (AIP) p11
Hauser M.G., Arendt R.G., Kelsall T., Dwek E., Odegard N., Weiland J.L. Freudenreich H.T., Reach W. et al. 1998, ApJ 508, 25
Heyl J., Colless M., Ellis R.S., Broadhurst T. 1997, MNRAS 285, 613
Helou G. 1986, ApJ 311, L33
Hughes D.H., Serjeant S., Dunlop J., Rowan-Robinson M., Blain A., Mann R.G., Ivison R., Peacock J. et al. 1998, Nature 394, 241
Joint IRAS Science Working Group 1985, IRAS Point Source Catalog (GPO, Washington DC)
Kawada M. 1998, in Proc. SPIE, Infrared Astronomical Instrumentation in press
Kawara K., Sato Y., Matsuhara H., Taniguchi Y., Okuda H., Sofue Y., Matsumoto T., Wakamatsu K. et al. 1998, A&A 336, L9
Kennicutt R.C. Jr, Tamblyn P., Congdon C.W. 1994, ApJ 435, 22
Kessler M.F., Steinz J.A., Anderegg M.E., Clavel J., Drechsel G., Estaria P., Faelker J., Riedinger J.R. et al. 1996, A&A 315, L27
Kinney A.L., Bohlin R.C., Calzetti D., Panagia N., Wyse R.F.G. 1993, ApJS 86, 5
Kinney A.L., Calzetti D., Bohlin R.C., McQuade K., Storchi-Bergmann T., Schmitt H.R. 1996, ApJ 467, 38
Lilly S.J., Tresse L., Hammer F., Crampton D., Le Fèvre O. 1995, ApJ 455, 108
Madau P., Ferguson H.C., Dickinson M.E., Giavalisco M., Steidel C.C., Fruchter A. 1996, MNRAS 283, 1388
Oke J.B., Gunn J.E. 1983, ApJ 266, 713
Pearson C. 1996, PhD Thesis, Imperial College of Science Technology & Medicine, London
Pearson C., Rowan-Robinson M. 1996, MNRAS 283, 174
Puget J.-L., Abergel A., Bernard J.-P., Boulanger F., Burton W.B., Désert F.-X., Hartmann D. 1996, A&A 308, L5
Rieke G.H., Lebofsky M.J. 1986, ApJ 304, 326
Rowan-Robinson M., Crawford J. 1989, MNRAS 238, 523
Sanders D.B., Mirabel I.F. 1996, ARA&A 34, 749
Saunders W., Rowan-Robinson M., Lawrence A., Efstathiou G., Kaiser N., Ellis R.S., Frenk C.S. 1990, MNRAS 242, 318
Schmitt H.R., Kinney A.L., Calzetti D., Storchi-Bergmann T. 1997, AJ 114, 592
Seaton M.J. 1979, MNRAS 187, L73
Smail I., Ivison R.J., Blain A.W. 1997, ApJ 490, L5
Small T.A., Sargent W.L.W., Hamilton D. 1997, ApJ 487, 512

Soifer B.T., Houck J.R., Neugebauer G. 1987a, ARA&A 25, 187

Soifer B.T., Sanders D.B., Madore B.F., Neugebauer G., Danielson G.E., Elias J.H., Lonsdale C.J., Rice W.L. 1987b, ApJ 320, 238

Spinoglio L., Malkan M.A., Rush B., Carrasco L., Recillas-Cruz E. 1995, ApJ 453, 616

Steidel C.C., Giavalisco M., Pettini M., Dickinson M., Adelberger K.L. 1996, ApJ 462, L17

Takeuchi T.T., Hirashita H., Ohta K., Hattori T.G., Ishii T.T., Shibai H. 1999a, PASP in press (T99)

Takeuchi T.T., Hirashita H., Ohta K., Ishii T.T., Yoshikawa K., Shibai H. 1999b, The Institute of Space and Astronautical Science Report in press